Comparison of the ^{7}Li(^{18}O,^{17}N)^{8}Be and ^{18}O(d,^{3}He)^{17}N reactions

A. T. Rudchik,[1,*] Yu. M. Stepanenko,[1] K. W. Kemper,[2] A. A. Rudchik,[1] O. A. Ponkratenko,[1] E. I. Koshchy,[3] S. Kliczewski,[4] K. Rusek,[5,6] A. Budzanowski,[4] S. Yu. Mezhevych,[1] I. Skwirczyńska,[4] R. Siudak,[4] B. Czech,[4] A. Szczurek,[4] J. Choiński,[6] and L. Głowacka[7]

[1]*Institute for Nuclear Research, Prospect Nauki 47, 03680 Kiev, Ukraine*
[2]*Physics Department, Florida State University, Tallahassee, Florida 32306-4350, USA*
[3]*Kharkiv National University, Svobody 4, 61077 Kharkiv, Ukraine*
[4]*H. Niewodniczański Institute of Nuclear Physics, Radzikowskiego 152, PL-31-342 Cracow, Poland*
[5]*A. Soltan Institute for Nuclear Studies, Hoża 69, PL-00-681 Warsaw, Poland*
[6]*Heavy Ion Laboratory, Warsaw University, L. Pasteura 5A, PL-02-093 Warsaw, Poland*
[7]*Institute of Applied Physics, Military University of Technology, Kaliskiego 2, PL-00-908 Warsaw, Poland*
(Received 5 September 2010; revised manuscript received 24 December 2010; published 15 February 2011)

New angular distributions for the ^{7}Li(^{18}O,^{17}N)^{8}Be reaction at an energy of $E_{\rm lab}(^{18}{\rm O}) = 114$ MeV for the ground states of ^{8}Be and ^{17}N and the excited states of ^{17}N were measured. These data and ^{18}O(d,^{3}He)^{17}N reaction data taken at $E_d = 52$ MeV were analyzed within the coupled-reaction-channels method using $^{7}{\rm Li} + {}^{18}{\rm O}$ and $^{18}{\rm O} + d$ optical potentials deduced from previous elastic and inelastic scattering results. Shell-model spectroscopic amplitudes were used in the analysis. Both reactions are dominated by single proton transfer. Calculations show that heavy-ion reactions of the type studied in this work can be used to identify final-state spins when measurements are carried to small angles.

DOI: 10.1103/PhysRevC.83.024606 PACS number(s): 25.70.Hi, 25.70.Bc, 24.10.Eq, 24.10.Ht

I. INTRODUCTION

Our understanding of the extraction of single-particle spectroscopic information as a function of depth of the orbit below the nuclear Fermi surface is a lively topic of study at present [1,2]. The current ability to investigate nuclei with large neutron or proton excesses through single-nucleon removal reactions means that theories of structure and reactions are being tested in relatively uncharted nuclear domains. It is difficult to probe this question with stable beams because the most easily accessible orbits are not deeply bound. However, it is possible, for example, that the use of proton pickup reactions with vastly different Q values from neutron-rich isotopes such as ^{18}O and ^{22}Ne can provide tests of current theories used in the more exotic rare isotope works. A recent experiment that bombarded a ^{7}Li target with an ^{18}O beam yielded a rich data set, one part of which, proton pickup, allows comparison between a standard light-ion reaction having a very negative Q value, with a heavy-ion reaction with a positive Q value.

The present work reports angular distributions for the ^{7}Li(^{18}O,^{17}N)^{8}Be reaction at the energy $E_{\rm lab}(^{18}{\rm O}) = 114$ MeV. This reaction was measured simultaneously with $^{7}{\rm Li} + {}^{18}{\rm O}$ elastic scattering [3] so that combining the deduced $^{7}{\rm Li} + {}^{18}{\rm O}$ potential parameters with shell-model spectroscopic amplitudes of nucleons and clusters, previously calculated, in a coupled-reaction-channels (CRC) analysis resulted in a detailed test of our interpretation of the ^{7}Li(^{18}O,^{17}N)^{8}Be reaction data. A further test of the spectroscopic amplitudes used in this study was carried out by their use in a CRC analysis of previously reported ^{18}O(d,^{3}He)^{17}N reaction data taken at $E_d = 52$ MeV [4]. The reaction Q value for the ^{7}Li(^{18}O,^{17}N)^{8}Be reaction is $+1.3$ MeV, while for the ^{18}O(d,^{3}He)^{17}N reaction, it is -10.5 MeV, so that different nuclear properties are probed in this comparison.

The paper is organized as follows. In Sec. II, we present the experimental procedure. The results of the CRC analysis of the ^{7}Li(^{18}O,^{17}N)^{8}Be and ^{18}O(d,^{3}He)^{17}N reaction data are presented. Comparison with the previously obtained potentials $^{8}{\rm Be} + {}^{15}{\rm N}$ [5], $^{8}{\rm Be} + {}^{13}{\rm C}$ [6], $^{8}{\rm Be} + {}^{9}{\rm Be}$ [7], and $^{8}{\rm Li} + {}^{17}{\rm O}$ [8] are also given in Sec. III. Summary and conclusions close our paper.

II. EXPERIMENTAL PROCEDURE

The present ^{7}Li(^{18}O,^{17}N)^{8}Be reaction data were taken at the same time as the previously reported ^{7}Li(^{18}O,^{18}O)^{7}Li elastic scattering data [3] at the Warsaw Heavy Ion Cyclotron Laboratory, which provided the 114-MeV ^{18}O beam for the experiment. The details of the target, detector, and data accumulation system are given in Ref. [3].

Figure 1 shows a typical $\Delta E(E)$ spectrum from the Si telescope used to collect the data. As can be seen, the resolution is sufficiently good to separate the reaction products of interest. Figure 2 shows a typical residual energy spectrum of ^{17}N from the ^{7}Li(^{18}O,^{17}N)^{8}Be reaction after subtraction of a background. To extract the yields, the peaks were fitted by the sum of Gauss symmetric functions

$$N(E) = \sum_i N_{0i} \exp\left(-0.5 \frac{(E - E_{0i})^2}{h_i^2} \right), \qquad (1)$$

with the peak positions E_i determined by the corresponding kinetic energies and by fixing the parameters h_i to the width of the elastic-scattering peaks or to the natural level width (curves in Fig. 2). The peak areas were used to calculate the reaction

*rudchik@kinr.kiev.ua

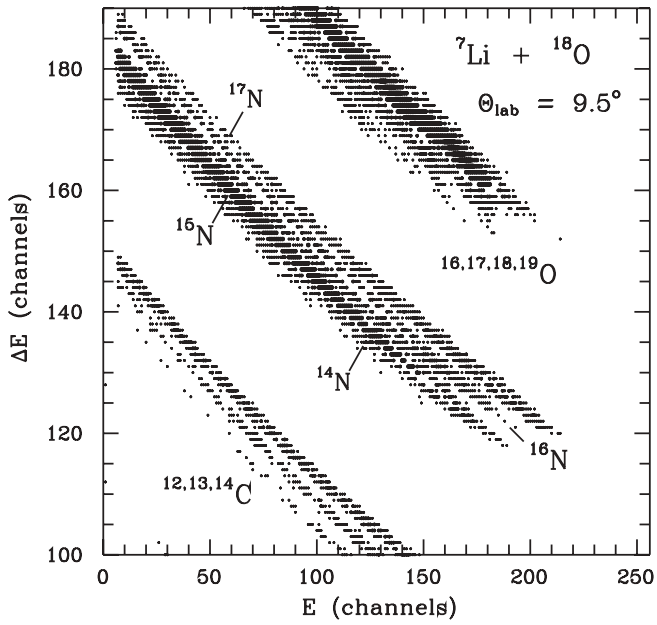

FIG. 1. Typical $\Delta E(E)$ spectrum of the products from ^{7}Li(^{18}O,X) reactions at energy $E_{lab}(^{18}O) = 114$ MeV.

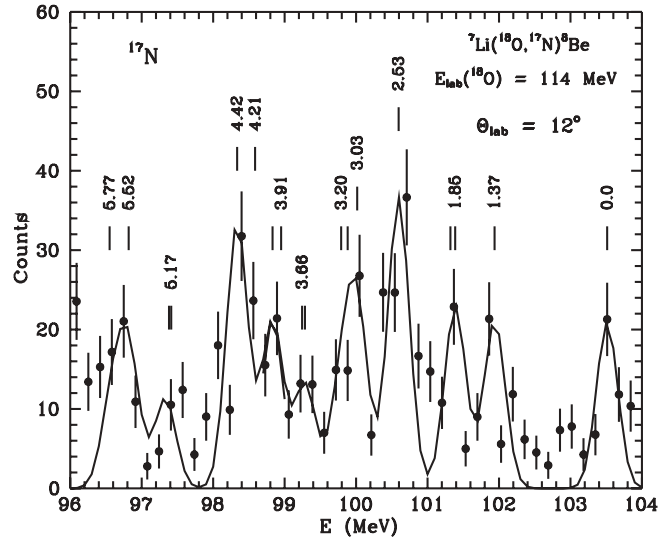

FIG. 2. Typical energy spectra of ^{17}N from the ^{7}Li(^{18}O,^{17}N)^{8}Be reaction at $E_{lab}(^{18}O) = 114$ MeV for the angle $\theta_{lab} = 11^\circ$ after subtraction of a background. The curves show the Gauss symmetric forms.

cross sections for the ground states of ^{8}Be and ^{17}N and excited states of ^{17}N. The area errors of peaks were estimated to be about 20% if the peaks were well resolved, and 30–40% for poorly resolved peaks.

The absolute cross sections for the ^{7}Li(^{18}O,^{17}N)^{8}Be angular distributions were obtained by multiplying them by the same normalization factor as determined from the simultaneously measured ^{7}Li + ^{18}O elastic scattering [3]. The error in the absolute cross section is about 15%. The resulting angular distributions of the ^{7}Li(^{18}O,^{17}N)^{8}Be reaction for ground states of ^{8}Be and ^{17}N and excited states of ^{17}N at energy $E_{lab}(^{18}O) =$ 114 MeV are shown in Figs. 3–6.

TABLE I. Parameters of optical potentials.

Nuclei	$E_{c.m.}$ (MeV)	E^* (MeV)	V_0 (fm)	r_V (MeV)	a_V (fm)	W_S (MeV)	r_W (fm)	a_W (fm)	Ref.
^{7}Li + ^{18}O	31.9	g.s.	174.5	0.806	0.900	13.0	1.470	0.900	[3]
^{8}Be + ^{17}N	33.2		174.5	0.800	0.900	7.0	1.250	0.900	
^{8}Li + ^{17}O	25.9		183.9	0.802	0.700	5.0	1.200	0.700	[8]
^{8}Be + ^{15}N	29.2		252.6	0.796	0.400	4.3	1.250	0.400	[5]
^{8}Be + ^{9}Be	24.8		192.4	0.788	0.678	9.0	1.600	0.678	[7]
^{8}Be + ^{13}C	31.1		170.2	0.793	0.760	7.0	1.250	0.760	[6]
$^{16(14)}$N + α	51.0		160.8	0.904	0.535	27.6	0.904	0.390	[13]
^{17}N + ^{3}He	36.4		175.5	0.687	0.750	24.0	1.150	0.750	
	35.0	1.374	175.5	0.687	0.750	24.0	1.350	0.750	
	34.5	1.845	175.5	0.687	0.750	24.0	1.250	0.750	
	34.4	1.907	175.5	0.687	0.750	24.0	1.300	0.750	
	33.8	2.526	175.5	0.687	0.950	20.0	1.550	0.450	
	33.2	3.129, 3.204	175.5	0.687	0.750	24.0	1.650	0.750	
	32.7	3.629, 3.663	175.5	0.687	0.750	24.0	1.700	0.750	
	30.8	5.515	175.5	0.687	0.750	24.0	1.250	0.750	
	29.4	6.990	175.5	0.687	0.750	24.0	1.250	0.750	
^{18}O + d[a]	9.0		81.0	0.737	0.893	7.8	1.430	0.440	
	46.8		81.0	0.737	0.893	20.0	1.430	0.440	
^{16}O + d[b]	46.8		82.5	0.687	0.769	10.5	1.137	0.777	
$^{19(18)}$O + p	48.5		37.8	0.827	0.706	9.0	1.129	0.486	[13]

[a]From fitting the ^{18}O + d elastic scattering data at $E_{lab} = 10$ MeV [14].
[b]From fitting the ^{16}O + d elastic scattering data [15]. The parameters of the spin-orbit potential were taken from Ref. [15].

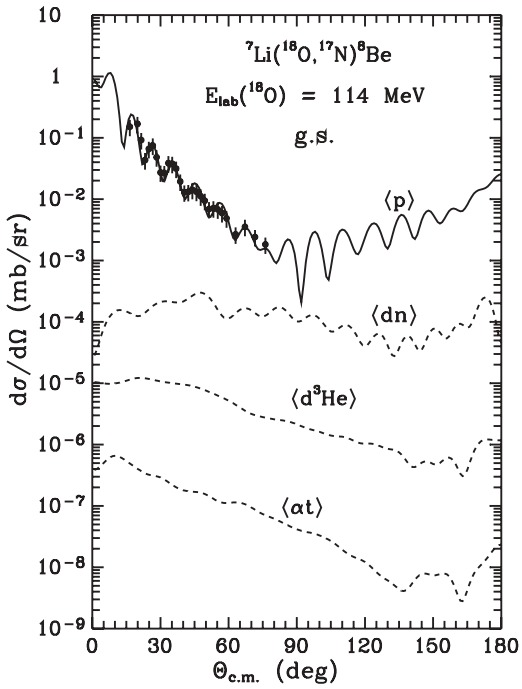

FIG. 3. Angular distribution of the ^{7}Li(^{18}O,^{17}N)^{8}Be reaction at $E_{lab}(^{18}O) = 114$ MeV for transition to the ground states of ^{8}Be and ^{17}N. The curves show the CRC calculations for different transfers.

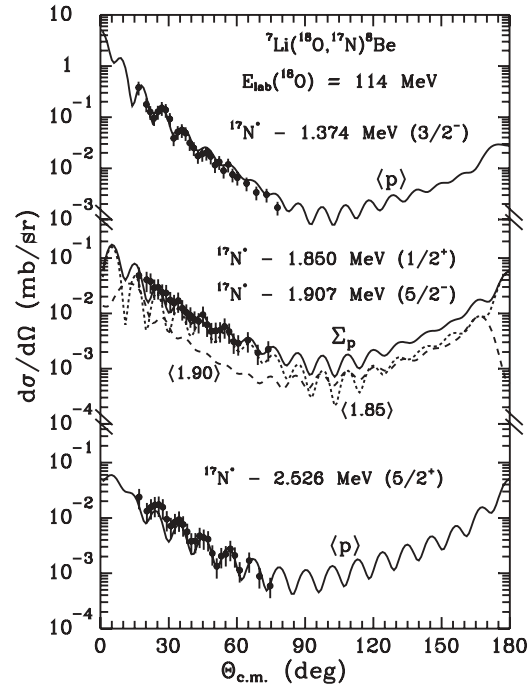

FIG. 4. Angular distribution of the ^{7}Li(^{18}O,^{17}N)^{8}Be reaction at $E_{lab}(^{18}O) = 114$ MeV for transitions to the 1.374 MeV (3/2^{-}), 1.850 MeV (1/2^{+}) + 1.907 MeV (5/2^{-}), and 2.526 MeV (5/2^{+}) states of ^{17}N. The curves show the CRC calculations for proton transfers.

III. THE DATA ANALYSIS

A. Calculation procedure

The reaction data were analyzed with the CRC method using optical model potentials in the entrance and exit channels of Woods-Saxon form

$$U(r) = V_0\left[1+\exp\left(\frac{r-R_V}{a_V}\right)\right]^{-1} + iW_S\left[1+\exp\left(\frac{r-R_W}{a_W}\right)\right]^{-1}, \quad (2)$$

and Coulomb potentials of a uniform charged sphere

$$V_C(r) = \begin{cases} \dfrac{Z_P Z_T e^2}{2R_C}\left(3-\dfrac{r^2}{R_C^2}\right), & r \leqslant R_C \\ \dfrac{Z_P Z_T e^2}{r}, & r > R_C. \end{cases} \quad (3)$$

Here

$$R_i = r_i\left(A_P^{1/3}+A_T^{1/3}\right), \quad i = V, W, C, \quad (4)$$

where A_P, Z_P and A_T, Z_T are the mass and charge numbers of ^{18}O,^{17}N and ^{7}Li, ^{8}Be, respectively; e is the electron charge. The parameter $r_C = 1.25$ fm was used in all calculations.

The most important transfer reactions as well as ^{7}Li + ^{18}O elastic and inelastic scattering were included in the coupled-channels scheme. The transitions to the excited states of ^{7}Li and ^{18}O were treated as in Ref. [3] (see Fig. 7 there). Figure 7 shows the diagrams of one- and two-step transfers, which were included in the calculations.

In the ^{7}Li + ^{18}O entrance reaction channel, the optical potential parameters obtained by fitting the elastic scattering data [3] were used. The ^{8}Be + ^{17}N potential was deduced from the experimental data by fitting the exit channel potential parameters

$$X_i = \{V_0, r_V, a_V, W_S, r_W, a_W\} \quad (5)$$

to the reaction data for ground and excited states of ^{17}N independently while keeping the ^{7}Li + ^{18}O potential parameters and the spectroscopic amplitudes S_x of transferred clusters or nucleons x fixed. The parameters of ^{7}Li + ^{18}O potential and ^{8}Be + ^{17}N potential parameters deduced in the fitting procedure are listed in Table I. The spectroscopic amplitudes S_x of transferred clusters or nucleons x for a nucleus $A = C + x$,

$$S_x = \binom{A}{x}^{1/2}\langle\Psi_A|\Psi_C\Psi_x;\varphi_{Cx}\rangle, \quad (6)$$

were obtained within the translationally invariant shell model (TISM) [9] by using the code DESNA [10,11]. The calculated values of amplitudes S_x are listed in the Appendix.

The wave function of x for a nucleus $A = C + x$ was calculated by varying the depth of the Woods-Saxon binding potential to reproduce the binding energy of x in nucleus A. The geometry parameters of the binding potentials were the following: $a = 0.65$ fm and $r_V = 1.25A^{1/3}/(C^{1/3}+x^{1/3})$ fm. The code FRESCO [12] was used for the CRC calculations. The description of the CRC method used is included in Ref. [12].

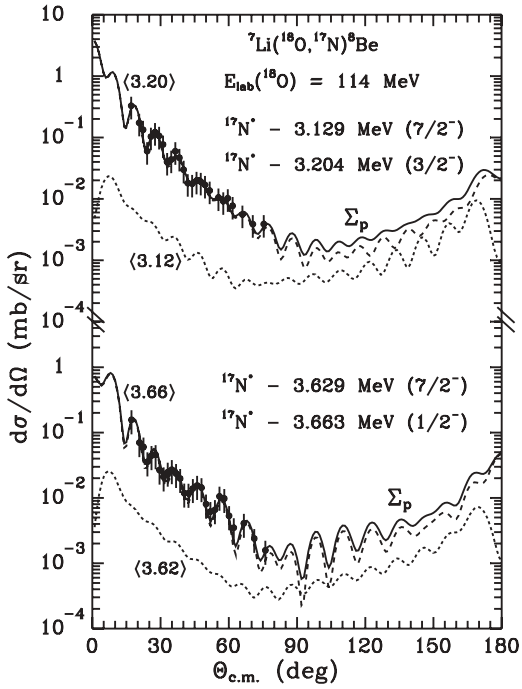

FIG. 5. Same as in Fig. 4, but for other excited states of ^{17}N.

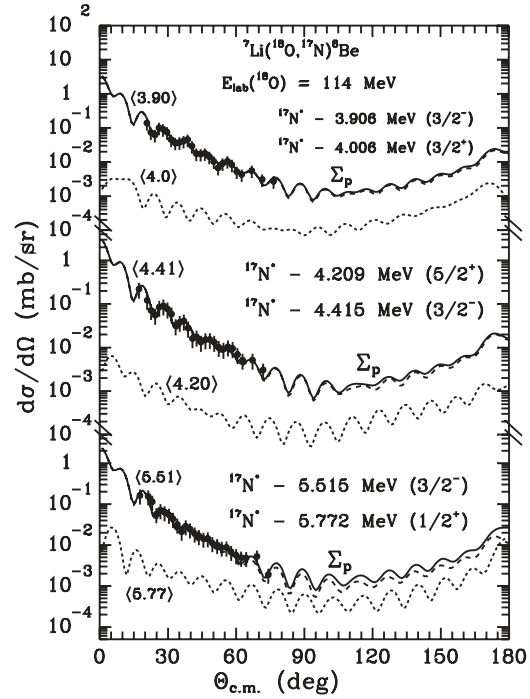

FIG. 6. Same as in Fig. 4, but for other excited states of ^{17}N.

B. ^{7}Li(^{18}O,^{17}N)^{8}Be reaction

The measured angular distribution of the ^{7}Li(^{18}O,^{17}N)^{8}Be reaction at $E_{lab}(^{18}O) = 114$ MeV leading to the ground states of ^{8}Be and ^{17}N and the results of the corresponding CRC calculations are presented in Fig. 3. The dashed curves labeled $\langle x \rangle$ show the CRC calculations for the direct transfers of particle x; those labeled $\langle xy \rangle$ present a coherent sum of two-step transfers of particles: first x and then y as well as vice versa. The proton transfer (curve $\langle p \rangle$) dominates. Other transfers contribute negligibly to this reaction.

Figures 4–6 show the angular distributions of the ^{7}Li(^{18}O,^{17}N*)^{8}Be reaction for transitions to different excited states of ^{17}N. As in the previous case, the proton transfer (curves $\langle p \rangle$ and Σ_p) dominates all transitions.

In Figs. 4–6, the curves Σ_p show the incoherent sums of the individual CRC calculations for the ^{7}Li(^{18}O,^{17}N*)^{8}Be reaction for the transitions to the excited states of ^{17}N unresolved in the experiment.

The proton transfer from the ground state of ^{18}O to ^{7}Li is forbidden for some excited states of ^{17}N*, i.e., spectroscopic amplitude $S_p = 0$ for such systems $^{18}\text{O} = {}^{17}\text{N}^* + p$. In these cases, the two-step processes were used, when the nucleus ^{18}O is excited to a level from which a proton transfer is possible (second diagram in Fig. 7), i.e., the spectroscopic amplitudes S_p for systems $^{18}\text{O}^* = {}^{17}\text{N}^* + p$ were used (see Table II in the Appendix). Such two-step proton transfers were used for the transitions to the 1.85 MeV ($1/2^+$), 1.907 MeV ($5/2^-$), 2.526 MeV ($5/2^+$), 3.129 MeV ($7/2^-$), 3.629 MeV ($7/2^-$), 4.006 MeV ($3/2^+$), 4.209 MeV ($3/2^+$), and 5.772 MeV ($1/2^+$) states of ^{17}N.

The $^8\text{Be} + {}^{17}\text{N}^*$ potential parameters deduced by fitting the ^{7}Li(^{18}O,^{17}N*)^{8}Be reaction data for the transitions to excited states of ^{17}N were found the same as for the ground state of ^{17}N.

In Table I, the $^8\text{Be} + {}^{17}\text{N}$ potential parameters are compared with those for the ^{8}Be interaction with ^{15}N, ^{13}C, and ^{9}Be as well as with the $^8\text{Li} + {}^{17}\text{O}$ potential parameters. The comparison of the $^8\text{Be} + {}^{17}\text{N}$ potential with those for $^8\text{Be} + {}^{15}\text{N}$ and $^8\text{Li} + {}^{17}\text{O}$ is shown also in Fig. 8. The $^8\text{Be} + {}^{17}\text{N}$ potential has the largest radial extent of all systems studied to date.

An interesting difference between the use of a reaction like (^{7}Li, ^{8}Be) and that of proton transfer with light ions is the possibility of determining final-state spins from small-angle cross section determinations. Early on in the study of heavy-ion transfer reactions [16,17] it was observed that transfers from a $p_{3/2}$ particle in the beam to a $p_{3/2}$ orbit in the target, resulted in a large cross section at small angles because of the presence of an allowed $L = 0$ component in

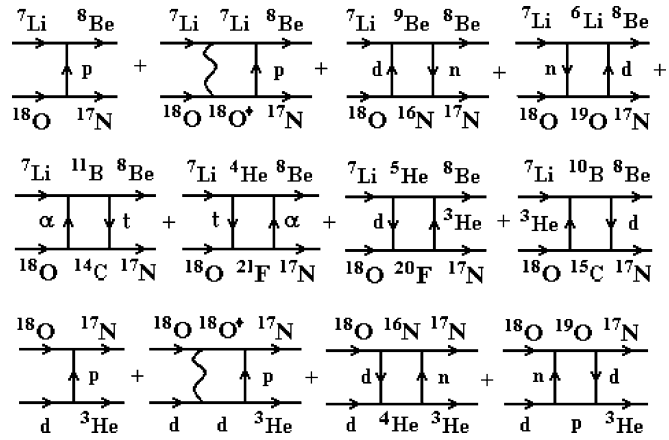

FIG. 7. Diagrams of different mechanisms of the ^{7}Li(^{18}O,^{17}N)^{8}Be and ^{18}O(d,^{3}He)^{17}N reactions.

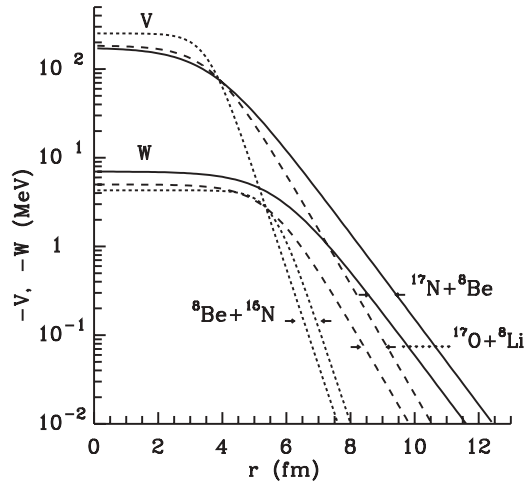

FIG. 8. Comparison of the ^{8}Be + ^{17}N, ^{8}Be + ^{15}N, and ^{8}Li + ^{17}O potentials.

the transferred angular momenta ($L = 0$, 1, 2), whereas that between a $p_{3/2}$ orbit and a $p_{1/2}$ one had a decreasing cross section at small angles ($L = 1$, 2). The appearance of this difference in angular distributions can be seen by comparing the calculations to the ground $1/2^-$ and $3/2^-$ first excited states in ^{17}N shown in Figs. 3 and 4. It is also possible to use beam-target combinations where the transferred particle is from either a $p_{3/2}$ or $p_{1/2}$ orbit to get the same type of cross section selectivity for determining final-state total spins in the nuclei of interest [18]. The use of inverse kinematics in the present work with Si detectors makes it difficult to carry out the present small-angle measurements needed to observe this final-state J dependence. However, were these measurements carried out with a modern spectrometer, it would be quite easy to distinguish the different final-state total spins up through the f-p shell [16,17]. Experimenters would have to resort to polarized beams or targets to get the same information from light-ion induced reactions.

C. ^{18}O(d,^{3}He)^{17}N reaction

The availability of previously published high-quality data for the ^{18}O(d,^{3}He) reaction at 52 MeV allows detailed testing of the spectroscopic amplitudes used in the heavy-ion reaction analysis of the previous section and makes possible a detailed comparison between two very different proton transfer reactions. The existence of ^{16}O + d elastic scattering data at 52 MeV means that the potential parameters needed for the ^{18}O(d,^{3}He)^{17}N reaction analysis can be determined from a fit to these data. The potential parameters are given in Table I, and the data and optical model (OM) calculations are shown in Fig. 9. The spin-orbit potential was taken from Ref. [15]. These parameters when combined with the previously calculated spectroscopic amplitudes leaves then as the only unknown in the reaction analysis the ^{3}He + ^{17}N potential parameters, which then are found from the CRC calculations. The diagrams for proton transfer in the (d,^{3}He) reaction are shown at the bottom of Fig. 7.

As an aside to the present analysis, the existence of ^{18}O + d elastic scattering data at 10 MeV allowed the potential parameter dependence of this elastic scattering to be explored over a wide energy range. It was found that a quite good description of the 10-MeV data could be found by simply reducing the strength of the imaginary potential from 20 to 7.8 MeV. The results of the calculation are shown in Fig. 9, and the parameter set is given in Table I.

In the CRC transfer analysis, the spectroscopic amplitudes were taken from Table II. For proton transfer via ^{18}O excitations, the collective model with deformation parameters from Ref. [3] was used for transitions to excited states in ^{17}N. The two-step transfers of $d + n$ and $n + d$ were calculated using ^{18}O + p potential parameters for the ^{19}O + p channel and the ^{14}N + α potential parameters from Ref. [13] for the ^{16}N + α channel. These sets of parameters are given in Table I. The ^{17}N + ^{3}He scattering potentials were found from fitting the ^{18}O(d,^{3}He)^{17}N reaction data and are listed in Table I.

Figure 10 shows the angular distributions of the ^{18}O(d,^{3}He)^{17}N reaction [4] and their corresponding CRC calculations. In Fig. 10, the curve $\langle dn \rangle$ shows the CRC calculations for the $d + n$ and $n + d$ transfers (coherent sum) for the transition to the ground state of ^{17}N. As one can see, these more exotic transfers give a small contribution to the (d,^{3}He) reaction, again demonstrating that the (d,^{3}He) transfer to the single-particle states proceeds as a one-step direct transfer. The fact that the present CRC analysis and the previous distorted-wave born approximation (DWBA) one of the (d,^{3}He) reaction both arrive at the conclusion that this reaction is dominated by one-step proton transfer gives strong support for the use of the DWBA when analyzing proton

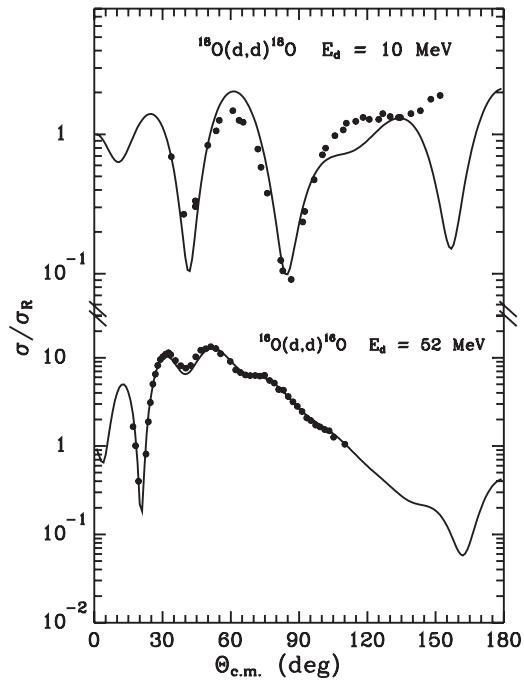

FIG. 9. Angular distribution of ^{18}O + d scattering at E_d = 10 MeV [14] and ^{16}O + d scattering at $E_d = 52$ MeV [15]. The curves are the OM calculations.

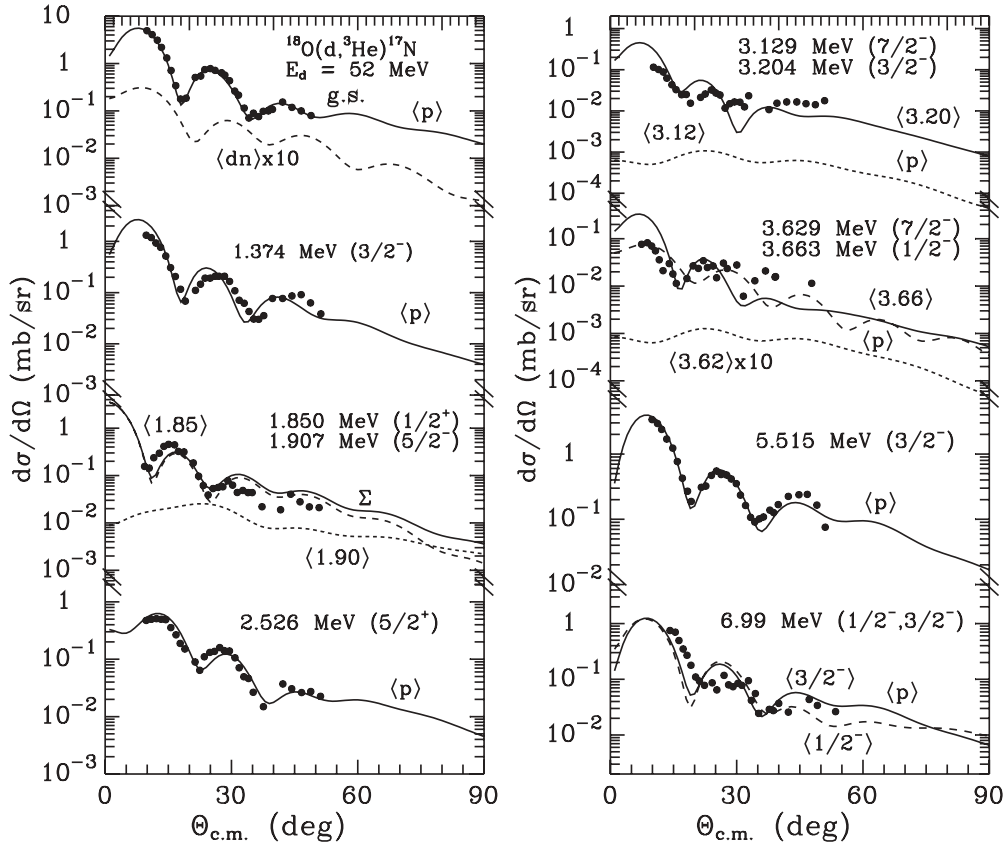

FIG. 10. Angular distribution of the ^{18}O(d,^{3}He)^{17}N reaction at $E_d = 52$ MeV [4]. Curves are the CRC calculations. Curves $\langle E \rangle$ ($E = 1.85$, 1.90, 3.12, 3.20, 3.62, 3.66) show CRC calculations for corresponding excited states of ^{17}N in MeV. Curves $\langle 1/2^- \rangle$ and $\langle 3/2^- \rangle$ show the calculations to the $1/2^-$ and $3/2^-$ states of ^{17}N, respectively. Curve $\langle dn \rangle$ shows the $d+n$, $n+d$ transfers (coherent sum).

pickup reactions in this energy range. These transfers are denoted in Fig. 10 by the curves $\langle p \rangle$.

The transitions dominated by single-proton transfer are to the $1/2^-$, $3/2^-$, $1/2^+$, and $5/2^+$ states in ^{17}N. The transitions to the $5/2^-$ and $7/2^-$ states in ^{17}N proceed via the 2^+ and 4^+ excited states in ^{18}O. In general, all transitions reported in the (d,^{3}He) work of Ref. [4] are satisfactorily described in the present work.

IV. SUMMARY AND CONCLUSIONS

The present work reports new data and an analysis of the proton transfer reaction ^{7}Li(^{18}O,^{17}N)^{8}Be and a reanalysis, with the same spectroscopic amplitudes as for the heavy-ion reaction, of previously reported ^{18}O(d,^{3}He)^{17}N. The success in describing the angular distributions for both reactions with the same single-proton spectroscopic strengths, even though they have radically different Q values, lends support to the idea that the reaction analysis carried out is well grounded with current reaction theory. It is also interesting that in the present case, while the reaction Q values are quite different in the two cases studied, the angular momenta mismatches are roughly the same (about 1 $\hbar$) and are well matched for the states populated in ^{17}N. Both reactions appear to be well described as single-proton transfers and can serve as test cases for future reaction theory studies. The present heavy-ion transfer calculations demonstrate the possible usefulness of these reactions for determining final-state total angular momenta in future studies with radioactive beams at laboratories that have modern magnetic spectrometers for small-angle measurements.

As part of the present analysis, optical potentials were deduced from the reaction analyses for both the ^{17}N + ^{8}Be and ^{17}N + ^{3}He systems. The ^{17}N + ^{8}Be real and imaginary potentials are stronger at larger radii than that for the ^{15}N + ^{8}Be system, suggesting that the lower breakup energy for ^{17}N ($\sim$5.8 MeV) and greater low-lying level density when compared with ^{15}N ($\sim$10.2 MeV) produces nuclear interactions at much greater distances than might be expected from the study of other systems.

ACKNOWLEDGMENTS

We thank Professor A. Sobiczewski, Professor J. Jastrzebski, and Dr. A. G. Artukh (JINR, Dubna, Russia) for their interest in this work. One of us (K.W.K.) acknowledges support of the State of Florida in this work.

APPENDIX

TABLE II. Spectroscopic amplitudes S_x of the particles x in the $A = C + x$ systems.

A	C	x	nL_j	S_x	A	C	x	nL_j	S_x
^{2}H	p	n	$1S_{1/2}$	−1.000	^{18}O$^{*}_{6.198}$	^{17}N$^{*}_{1.850}$	p	$1P_{1/2}$	−0.393
^{3}He	p	d	$1S_{1}$	−1.225[a]				$1P_{3/2}$	−0.556[a]
^{3}He	d	p	$1S_{1/2}$	1.225[a]	^{18}O$^{*}_{1.982}$	^{17}N$^{*}_{1.907}$	p	$1P_{1/2}$	0.279[a]
^{4}He	d	d	$1S_{1}$	1.732	^{18}O$^{*}_{3.555}$	^{17}N$^{*}_{1.907}$	p	$1P_{3/2}$	0.976
^{4}He	^{3}He	n	$1S_{1/2}$	1.414[a]	^{18}O$^{*}_{3.920}$	^{17}N$^{*}_{1.907}$	p	$1P_{1/2}$	0.279[a]
^{7}Li	^{4}He	t	$2P_{3/2}$	−1.091				$1P_{3/2}$	−0.149
^{7}Li	^{5}He	d	$2S_{1}$	−0.674[a]	^{18}O$^{*}_{5.255}$	^{17}N$^{*}_{1.907}$	p	$1P_{1/2}$	0.279[a]
			$1D_{1}$	−0.121[a]				$1P_{3/2}$	−0.149
			$1D_{3}$	0.676[a]	^{18}O	^{17}N$^{*}_{2.526}$	p	$1D_{5/2}$	−1.173[a]
^{7}Li	^{6}Li	n	$1P_{1/2}$	−0.657	^{18}O$^{*}_{4.450}$	^{17}N$^{*}_{2.526}$	p	$1P_{3/2}$	−1.179[a]
			$1P_{3/2}$	−1.179[a]	^{18}O$^{*}_{5.098}$	^{17}N$^{*}_{2.526}$	p	$1P_{3/2}$	0.629
^{8}Be	^{5}He	^{3}He	$2P_{3/2}$	−1.102[a]	^{18}O$^{*}_{6.198}$	^{17}N$^{*}_{2.526}$	p	$1P_{3/2}$	−0.735[a]
^{8}Be	^{4}He	α	$3S_{0}$	1.225	^{18} O$^{*}_{6.404}$	^{17}N$^{*}_{2.526}$	p	$1P_{3/2}$	0.629[a]
^{8}Be	^{6}Li	d	$2S_{1}$	1.217	^{18}O$^{*}_{3.555}$	^{17}N$^{*}_{3.129}$	p	$1P_{1/2}$	−0.861
^{8}Be	^{7}Li	p	$1P_{3/2}$	1.234[a]				$1P_{3/2}$	−0.727[a]
^{9}Be	^{7}Li	d	$2S_{1}$	−0.226[a]	^{18}O	^{17}N$^{*}_{3.204}$	p	$1P_{3/2}$	−1.217[a]
			$1D_{1}$	0.111[a]	^{18}O$^{*}_{1.982}$	^{17}N$^{*}_{3.204}$	p	$1P_{1/2}$	0.302
			$1D_{3}$	−0.624[a]				$1P_{3/2}$	0.302[a]
^{9}Be	^{8}Be	n	$1P_{3/2}$	0.866	^{18}O$^{*}_{3.920}$	^{17}N$^{*}_{3.204}$	p	$1P_{1/2}$	0.302
^{10}B	^{7}Li	^{3}He	$2P_{3/2}$	0.419				$1P_{3/2}$	0.302[a]
			$1F_{5/2}$	−0.104[a]	^{18}O$^{*}_{5.255}$	^{17}N$^{*}_{3.204}$	p	$1P_{1/2}$	0.302
			$1F_{7/2}$	0.347				$1P_{3/2}$	0.302[a]
^{10}B	^{8}Be	d	$1D_{3}$	0.811	^{18}O$^{*}_{3.555}$	^{17}N$^{*}_{3.629}$	p	$1P_{1/2}$	−0.861
^{11}B	^{7}Li	α	$3S_{0}$	−0.638				$1P_{3/2}$	−0.727[a]
			$2D_{2}$	−0.422	^{18}O	^{17}N$^{*}_{3.663}$	p	$1P_{1/2}$	1.198[a]
^{11}B	^{8}Be	t	$2P_{3/2}$	0.641	^{18}O$^{*}_{1.982}$	^{17}N$^{*}_{3.663}$	p	$1P_{3/2}$	−0.559
^{17}N	^{14}C	t	$1P_{1/2}$	0.466	^{18}O	^{17}N$^{*}_{3.906}$	p	$1P_{3/2}$	1.695[a]
^{17}N	^{15}C	d	$1P_{1}$	0.240[a]	^{18}O$^{*}_{4.456}$	^{17}N$^{*}_{4.006}$	p	$1P_{1/2}$	−0.439[a]
^{17}N	^{16}N	n	$1D_{3/2}$	−1.008				$1P_{3/2}$	0.196
^{17}N$^{*}_{1.374}$	^{16}N	n	$2S_{1/2}$	−0.713	^{18}O$^{*}_{4.456}$	^{17}N$^{*}_{4.209}$	p	$1P_{3/2}$	−0.589[a]
^{18}O	^{14}C	α	$4S_{0}$	−0.802	^{18}O	^{17}N$^{*}_{4.415}$	p	$1P_{3/2}$	1.695[a]
^{18}O	^{15}C	^{3}He	$3S_{1/2}$	−0.903[a]	^{18}O	^{17}N$^{*}_{5.515}$	p	$1P_{3/2}$	1.695[a]
^{18}O	^{16}N	d	$2P_{2}$	−1.304	^{18} O$^{*}_{4.456}$	^{17}N$^{*}_{5.770}$	p	$1P_{1/2}$	−0.393
^{18}O	^{17}N	p	$1P_{1/2}$	1.198[a]				$1P_{3/2}$	−0.556[a]
^{18}O	^{17}N$^{*}_{1.374}$	p	$1P_{3/2}$	−1.217[a]	^{18}O	^{17}N$^{*}_{6.99}(1/2^{-})$	p	$1P_{1/2}$	1.198[a]
^{18}O$^{*}_{1.982}$	^{17}N$^{*}_{1.374}$	p	$1P_{1/2}$	0.559		^{17}N$^{*}_{6.99}(3/2^{-})$	p	$1P_{3/2}$	−1.217[a]
			$1P_{3/2}$	0.559[a]	^{19}O	^{17}N	d	$1F_{2}$	−0.209
^{18}O$^{*}_{3.920}$	^{17}N$^{*}_{1.374}$	p	$1P_{1/2}$	0.559				$1F_{3}$	−0.056[a]
			$1P_{3/2}$	0.559[a]	^{19}O	^{18}O	n	$1D_{5/2}$	−0.882
^{18}O$^{*}_{5.255}$	^{17}N$^{*}_{1.374}$	p	$1P_{1/2}$	0.559	^{20}F	^{17}N	^{3}He	$3P_{3/2}$	−0.103
			$1P_{3/2}$	0.559[a]				$2F_{5/2}$	−0.105
^{18}O	^{17}N$^{*}_{1.850}$	p	$2S_{1/2}$	−0.453[a]	^{20}F	^{18}O	d	$2D_{2}$	0.380
^{18}O$_{*4.456}$	^{17}N$^{*}_{1.850}$	p	$1P_{1/2}$	−0.393	^{21}F	^{17}N	α	$3F_{3}$	0.059
			$1P_{3/2}$	−0.556[a]	^{21}F	^{18}O	t	$3D_{5/2}$	−0.001

[a] $S_{\mathrm{FRESCO}} = (-1)^{J_C+j-J_A} S_x = -S_x$.

[1] A. Gade *et al.*, Phys. Rev. C **77**, 044306 (2008).
[2] J. Lee *et al.*, Phys. Rev. Lett. **104**, 112701 (2010).
[3] A. A. Rudchik *et al.*, Nucl. Phys. A **785**, 293 (2007).
[4] D. Hartwig *et al.*, Z. Phys. **246**, 418 (1971).
[5] A. A. Rudchik *et al.*, Eur. Phys. J. A **23**, 445 (2005).
[6] A. T. Rudchik *et al.*, Nucl. Phys. A **660**, 267 (1999).
[7] V. O. Romanyshyn *et al.*, Phys. Rev. C **79**, 054609 (2009).
[8] A. T. Rudchik *et al.*, Nucl. Phys. A **831**, 139 (2009).
[9] Yu. F. Smirnov and Yu. M. Tchuvil'sky, Phys. Rev. C **15**, 84 (1977).
[10] A. T. Rudchik and Yu. M. Tchuvil'sky, computer code DESNA, Report KIYAI-82-12, Institute for Nuclear Research, Ukrainian Academy of Science, Kiev, 1982 (unpublished).
[11] A. T. Rudchik and Yu. M. Tchuvil'sky, Ukr. Phys. J. **30**, 819 (1985).

[12] I. J. Thompson, Comput. Phys. Rep. **7**, 167 (1988).
[13] C. M. Perey and F. G. Perey, At. Data Nucl. Data Tables **17**, 1 (1976).
[14] E. J. Stephenson *et al.*, Nucl. Phys. A **331**, 269 (1979).
[15] F. Hinterberger *et al.*, Nucl. Phys. A **111**, 265 (1968).
[16] R. L. White, K. W. Kemper, L. A. Charlton, and G. D. Gunn, Phys. Rev. Lett. **32**, 892 (1974).
[17] K. W. Kemper, R. L. White, L. A. Charlton, G. D. Gunn, and G. E. Moore, Phys. Lett. B **52**, 179 (1974).
[18] P. D. Bond, J. Barrette, C. Baktash, C. E. Thorn, and A. J. Kreiner, Phys. Rev. Lett. **46**, 1565 (1981).